Analysis of Downlink Connectivity in NB-IoT Networks Employing NOMA with Imperfect SIC

Shashwat Mishra, Lou Salaun, Chung Shue Chen, K Giridhar

Analysis of Downlink Connectivity in NB-IoT Networks Employing NOMA with Imperfect SIC

Shashwat Mishra[*†], Lou Salaün[†], Chung Shue Chen[†], K. Giridhar[*]
[*] Indian Institute of Technology (IIT) Madras, Chennai, India 600036
[†] Nokia Bell Labs, Paris-Saclay, 91620 Nozay, France
Email: {shashwat, giri}@tenet.res.in, {lou.salaun, chung_shue.chen}@nokia-bell-labs.com

***Abstract*—We study the problem of maximizing the number of served devices in a non-orthogonal multiple access (NOMA) based Narrowband Internet of Things (NB-IoT) network for supporting massive connectivity in the downlink. We analyze this problem under practical system limitations of imperfect successive interference cancellation (SIC) at the receiver along with data rate, power and bandwidth constraints. We propose a strategy for joint device and power allocation through an iterative solution for a system of linear equations on each sub-carrier that maximizes the number of connected devices. We evaluate the performance of the proposed solution over a wide range of service scenarios through extensive computer simulations and demonstrate the sensitivity of connectivity in power domain NOMA based NB-IoT systems to the residual interference resulting from imperfect SIC.**

***Keywords*—NB-IoT, NOMA, Connectivity Maximization, Imperfect SIC, mMTC, MTCD, 5G**

I. Introduction

The predominant demand from 5G and beyond (B5G) wireless communication networks is to accommodate a massive number of devices with diverse quality of service (QoS) requirements. The Cisco Visual index [1] reports that half of the global connected devices, about 14.7 billion entities, by 2023 will be machine-to machine (M2M) connections. M2M devices are communicating entities that do not necessarily need human interaction. This sharp increase in the number of machine type communication devices (MTCDs) is due to the advent of new deployment scenarios such as smart cities, automated factory floors, traffic monitoring, weather forecast and warning networks, agricultural automation, to name a few. To this end, the massive machine type communication (mMTC) use-case was introduced within 5G, where devices are characterized by high deployment density, moderate data rate, modest reaction time requirement and low transmit power.

The mMTC use-case is continuously evolving, with new technologies being regularly proposed, and with existing ones moving into new application domains [2], [3]. Out of the numerous enabling technologies, NB-IoT has emerged as a very promising candidate for increasing the density of connected device. NB-IoT has a high expected device density of about 52500 devices sending small payload in an area of 0.86 km^2 using 200 kHz of bandwidth with OFDMA, possibly deployed within pre-existing LTE deployments [4]. There is a rich background of research exploring NB-IoT deployments both in 4G as well as 5G networks [5].

However, it is becoming increasingly difficult to deploy dedicated bandwidth exclusively for NB-IoT use-cases due to massive growth of radio communication systems, so there is a need to develop solutions that can efficiently perform radio resource allocation to fulfill the service requirements [6]. With the advancements in device processing capabilities and semiconductor manufacturing efficiency, NOMA has now become a lucrative paradigm for accommodating a large number of devices in limited bandwidth resources through non-orthogonal resource allocation [7]. NOMA improves the spectral efficiency of a communication system through superposition coding at the transmitter and successive interference cancellation (SIC) at the receiver [8].

The authors in [9] show that power domain NOMA can be effectively employed for increasing user density in networks. However, this work assumes no restriction on the number of superimposed devices on each sub-carrier. But in practice superimposing a large number of devices in a NOMA system is impractical due to error propagation issues in SIC, signaling overhead and increased decoding complexity at the receiver. A crucial aspect of NOMA for achieving superior spectral efficiency is proper user signal superposition and power allocation which is examined in [10]. The authors in [11] address the optimal user grouping problem in the downlink to maximize the sum rate where it is shown that due to the combinatorial nature, the computational complexity to find the optimal solution is very high.

The use of NOMA to support mMTC communication and LPWA networks is a relatively new approach and it has gained a lot of attention in recent times [12]. The work in [13] presents a thorough comparison between popular LPWA network technologies for IoT and show that NB-IoT is especially lucrative due to its power efficiency and deep coverage capabilities. The key goal of mMTC use-case is ensuring massive connectivity. As such, considering the number of served devices as a performance evaluation metric of an mMTC deployment is better than other metrics like the network sum-rate, user fairness or device outage probability. However, the literature that addresses the problem of connectivity maximization for the evaluation of NB-IoT deployments, is very limited.

The works in [14], [15] consider a joint sub-carrier and power allocation problem to maximize the uplink connection density in NB-IoT NOMA networks while taking the QoS requirements and the transmit power constraints of IoT devices into account. The results of these works show that using NOMA in the uplink of NB-IoT networks provides significant gain in connectivity over the current state-of-the-art solutions in terms of connection density.

In practice, some residual interference invariably remains in the process of SIC. Furthermore, it is well known that even a small amount of this residual interference can severely affect a NOMA system's performance [16]–[19]. The impact of residual interference in the context on LPWA networks is studied through test-bed experiments in [20].

There is very limited literature that investigates the impact of imperfect SIC in the mMTC use-case. The work in [21] develops an analytical framework based on stochastic geometry to investigate the system performance in terms of average success probability and average number of simultaneously served MTCDs, under imperfect successive interference cancellation in the uplink. However, the work is limited to the analysis of the uplink mMTC in a large-scale cellular network system overlaid with data aggregators.

In our previous work [22], we proposed a connection density optimal sub-carrier and power allocation strategy, called stratified device allocation (SDA), assuming perfect CSI knowledge for all the devices at the BS. Additionally, we developed a stochastic framework for connectivity maximization when only the path-loss of the devices is known at the BS and propose solutions through convex optimization. However, there we assumed that perfect SIC can be performed at the receiver. Developing on top of the previous findings, this work examines the connectivity potential of NOMA under the existence of residual interference due to imperfect SIC. To the best of our knowledge, no downlink connectivity maximization problem has been studied in this setting. The main contributions of the paper can be summarized as follows:

1) We propose a joint device power allocation and sub-carrier assignment scheme that maximizes the number of devices achieving their QoS requirement, taking into account the impact of imperfect SIC.
2) We analyze the impact of residual interference due to imperfect SIC on NB-IoT NOMA under a wide range of service scenarios including various cell radius and QoS requirement.
3) We evaluate the sensitivity of connectivity in the above power domain NOMA against 3GPP OMA and offer implementation recommendation and key guideline for employing NOMA in the NB-IoT.

The rest of this paper is organized as follows. Section II describes the system model and NOMA framework used in this work. In Section III, we define the connectivity maximization problem under imperfect SIC. Subsequently in Section IV, we propose a solution to this problem through an iterative algorithm based on solving a system of linear equations for optimal device power assignment. We evaluate the performance of the proposed solution through computer simulations in Section V. Finally, Section VI concludes the paper.

II. System Model

We consider a set of D contending devices denoted by $\mathcal{D} \triangleq \{1, \ldots, D\}$ that are dropped randomly and uniformly in an area served by one base station (BS). Our aim is to maximize the number of devices achieving their QoS requirements in the downlink within a given power budget. We assume that the system's SIC limitation, i.e., the maximum number of superimposed devices on each sub-carrier is M. The system's power budget for one physical resource block (PRB) is limited to $P_{\max}$. Each PRB is divided into S sub-carriers, the set of which is denoted by $\mathcal{S} \triangleq \{1, \ldots, S\}$. The system has a bandwidth of B_s Hz with each sub-carrier of equal bandwidth B Hz. Each device can be allocated only one sub-carrier in the downlink [4]. We consider that thermal noise is additive, white and Gaussian distributed, denoted as $N \triangleq N_0 \cdot B \cdot 10^{\frac{F}{10}}$, where N_0 is noise spectral density measured in W/Hz, B is the bandwidth and F is the noise figure expressed in dB. We will assume that all devices face the same additive white Gaussian noise N.

A. NOMA Framework

In this work, we consider signal multiplexing in the power domain for connectivity maximization. Let there be devices $\{1, \ldots, i, \ldots, k\}$ where $k \leq M$ with messages $x_1, \ldots, x_i, \ldots, x_k$ respectively on a given sub-carrier. Then, the downlink received signal at device 1 can be expressed as:

$$y_1 = h_1 \left\{\sqrt{p_1}x_1 + \ldots + \sqrt{p_i}x_i + \ldots + \sqrt{p_k}x_k\right\} + N,$$

where p_i is the transmit power for device i and h_i represents its composite channel gain. This channel gain takes into account both path-loss and small-scale Rayleigh fading for device i. The channel is taken to be flat-fading since the system has narrow bandwidth. We assume, without loss of generality, that the devices are sorted in decreasing order of their channel gains. That is,

$$g_1 \geq \cdots \geq g_D, \tag{1}$$

where $g_i \triangleq |h_i|^2$ is the amplitude of the channel gain for device i. We denote the set of devices allocated to sub-carrier n by $\mathcal{D}_n$ and define vector $\boldsymbol{d}_n \triangleq (d_n(1), \ldots, d_n(D_n))$ to represent these devices, where $D_n \triangleq |\mathcal{D}_n| \leq M$, for all $n \in \mathcal{S}$, due to the SIC constraint. In downlink NOMA, the optimal decoding order on sub-carrier n for SIC is to follow the increasing order of the channel gains g_i, since a strong device can decode both its own signal and the signal for the interferer while a weaker device treats the other devices' signals as noise and can decode only its own signal [23]. Therefore, we assume that the $d_n(i)$'s are sorted as follows: $g_{d_n(1)} \geq \cdots \geq g_{d_n(D_n)}$. Consequently, $d_n(i)$ would be the $(D_n - i + 1)$-th decoded device on sub-carrier n. The SINR for device $d_n(i)$ in this system is given as:

$$\gamma_{d_n(i)} = \frac{g_{d_n(i)} p_{d_n(i)}}{I_{d_n(i)} + \tilde{I}_{d_n(i)} + N}, \tag{2}$$

where $I_{d_n(i)}$ is the interference to device $d_n(i)$ caused by the stronger devices on the same sub-carrier:

$$I_{d_n(i)} \triangleq g_{d_n(i)} \sum_{j=1}^{i-1} p_{d_n(j)}.$$

The device $d_n(i)$ cannot cancel this interference and treats it as noise while trying to decode its own signal. The term $\tilde{I}_{d_n(i)}$ represents the residual interference caused at $d_n(i)$ due to imperfect SIC for the weaker devices and can be represented as:

$$\tilde{I}_{d_n(i)} \triangleq g_{d_n(i)} \xi \sum_{j=i+1}^{D_n} p_{d_n(j)},$$

where $0 \leq \xi \leq 1$ denotes the fraction of residual power from the weak devices. Ideally, this term should be zero. However, due to the imperfect SIC operation in a practical system, this additional interference is inevitably present and can originate due to multiple factors such as asynchronization during signal reconstruction and subtraction [20], or phase and amplitude mismatch at the receiver hardware [18]. Throughout this work, we assume that ξ is a fixed value that is identical for all the devices. It is possible to obtain a reasonable estimate of ξ at the BS, for example through long term error vector magnitude measurements [24].

B. Problem Constraints

There are the following constraints to be considered in our system. First, we have the power budget:

$$0 \leq \sum_{n=1}^{S}\sum_{i=1}^{D_n} p_{d_n(i)} \leq P_{\max}. \tag{3}$$

Here, $P_{\max}$ is the maximum total transmit power. Additionally, each device must achieve a minimum critical data rate R to satisfy its QoS requirements. The achievable data rate for device $d_n(i)$ is given as:

$$r_{d_n(i)} = B \log_2\left(1 + \gamma_{d_n(i)}\right). \tag{4}$$

Alternatively, this service rate requirement can be written in the terms of the device's SINR using (2) as follows:

$$\gamma_{d_n(i)} \geq \zeta, \qquad \forall n \in \mathcal{S}, \forall i \in \boldsymbol{d}_n, \tag{5}$$

where $\zeta = 2^{R/B} - 1$.

III. Problem Formulation

We assume that the channel state information g_i, for any device $i \in \mathcal{D}$, is known perfectly at the BS. Let us define vector $\boldsymbol{p}_n \triangleq (p_{d_n(1)}, \ldots, p_{d_n(D_n)})$ to denote the powers of all devices on sub-carrier n, and vector $\boldsymbol{p} \triangleq (\boldsymbol{p}_n)_{n\in\mathcal{S}}$ to represent the list of the power vectors $\boldsymbol{p}_n$. We define $Z_n(\boldsymbol{p}_n, \boldsymbol{d}_n)$ as the number of connected devices on sub-carrier n:

$$Z_n(\boldsymbol{p}_n, \boldsymbol{d}_n) \triangleq \sum_{i=1}^{D_n} \mathbb{1}\left(\gamma_{d_n(i)} \geq \zeta\right). \tag{6}$$

Here, $\mathbb{1}\left(\gamma_{d_n(i)} \geq \zeta\right)$ is the indicator function that takes value 1 if the rate for device $d_n(i)$ is at least equal to the required service rate R, and 0 otherwise. Therefore, $Z_n(\boldsymbol{p}_n, \boldsymbol{d}_n)$ has the QoS constraint (5) implicitly enforced in its definition. Using (3), (5) and (6), the downlink connectivity maximization problem given perfect CSI can be stated as follows:

$$\begin{aligned} \underset{\forall n\in\mathcal{S},\, \boldsymbol{p}_n,\, \boldsymbol{d}_n}{\text{maximize}} \quad & \sum_{n=1}^{S} Z_n(\boldsymbol{p}_n, \boldsymbol{d}_n) && (\mathcal{P})\\ \text{subject to} \quad & C1: \ 0 \leq \sum_{n=1}^{S}\sum_{i=1}^{D_n} p_{d_n(i)} \leq P_{\max},\\ & C2: \ \sum_{n\in\mathcal{S}} |\{k\} \cap \mathcal{D}_n| \leq 1, \forall k \in \mathcal{D},\\ & C3: \ D_n \leq M, \forall n \in \mathcal{S}. \end{aligned}$$

The objective function in $\mathcal{P}$ aims to maximize the number of connected devices over all sub-carriers in $\mathcal{S}$ that satisfy their QoS requirement. Constraint C1 is system power budget. Constraint C2 implies that each device can be allocated one sub-carrier according to 3GPP NB-IoT [4]. Constraint C3 states the SIC limit of the system of supporting at most M devices superposed per sub-carrier. Additionally, the total bandwidth taken up by all the connected devices must be less than $M \cdot B_s$ and this condition is inherently enforced by C3 considering the sub-carrier bandwidth B.

IV. Proposed Algorithm

The connectivity maximization problem ($\mathcal{P}$) can be decomposed into two parts. The first part requires us to decide the allocation of devices, i.e., the SIC ordering on each sub-carrier. For this, we consider Algorithm 1, which was introduced in our previous paper [22]. On a given sub-carrier, it assigns devices in the decreasing order of the channel gain following (1). It has been proven that this device configuration is optimal in terms of connectivity, assuming SIC is perfect, i.e., when $\xi = 0$.

Algorithm 1 Device Allocation

Input: B, M, N, a set of devices $\mathcal{D}'$ and $g_d, \forall d \in \mathcal{D}'$

1: **Initialization:** $\forall n \in \mathcal{S}$, $\boldsymbol{d}_n \leftarrow \varnothing$, $i \leftarrow 1$
2: **for** layer $= 1$ to M **do**
3:     **for** $n = 1$ to S **do**
4:         **if** $i \leq |\mathcal{D}'|$ **then**
5:             $\boldsymbol{d}_n(\text{layer}) \leftarrow i$
6:             $i \leftarrow i + 1$
7:         **else**
8:             **return** $\forall n \in \mathcal{S}$, $\boldsymbol{d}_n$
9:         **end if**
10:     **end for**
11: **end for**

The second part of the connectivity maximization problem consists in optimizing the transmit power of the devices allocated in the first part. We propose an iterative power allocation algorithm that solves a system of linear equations on each of the sub-carriers so as to allocate the minimum power required by each device to achieve its data rate. This ensures that we can fit the maximum possible devices in the given power budget.

To begin with, we assume an initial configuration with M devices on as many sub-carriers as possible (see line 4 in Algorithm 1). With this configuration of devices, the power consumption of each device on a given sub-carrier can be evaluated using (2) by setting the value of $\gamma_{d_n(i)}$ equal to ζ. This condition ensures that only the minimum power required to satisfy the QoS constraint is allocated to each device. Thus the power allocation $\boldsymbol{p}_n$ for devices on sub-carrier n is can be elaborated as follows:

$$\boldsymbol{p}_n = A^{-1} C_n, \tag{7}$$

where the vector C_n is given as:

$$C_n = \left(\frac{\zeta N}{g_1}, \frac{\zeta N}{g_2}, \cdots, \frac{\zeta N}{g_{d_n}}\right), \tag{8}$$

and A is a matrix of constant factors given as:

$$A_{i,j} = \begin{cases} -\xi\zeta, & i < j,\\ 1, & i = j,\\ -\zeta, & i > j. \end{cases}$$

This power allocation paradigm is elaborated in Algorithm 2. We calculate the total power required by all the devices similarly by solving the system of equations shown in (7) on all the sub-carriers as shown on line 4 in Algorithm 2. On line 5, we check if constraint C1 of $\mathcal{P}$ is satisfied. Here, through the 1-norm $\|\boldsymbol{p}\|_1$, we represent the total power allocated to all the devices in the set $\mathcal{D}'$. If this power exceeds the power budget $P_{\max}$, we change the device configuration on the last sub-carrier such that the weakest device is excluded from allocation, as shown on lines 9-10. This procedure is repeated in the while loop (lines 3-10) until a set $\mathcal{D}'$ is found for which the total allocated power is less than the system's power budget $P_{\max}$. At termination, on line 7, the algorithm outputs the number of connected devices Z^*, the corresponding device allocation $\boldsymbol{d}_n$, $n \in \mathcal{S}$, and the power allocation $\boldsymbol{p}$.

Algorithm 2 Iterative Joint Device and Power Allocation

Input: B, M, N, $P_{\max}$ and $g_d, \forall d \in \mathcal{D}$

1: **Initialization:** $Z^* \leftarrow 0$, $\bar{Z} \leftarrow 0$
2: $\forall n \in \mathcal{S}$, $\boldsymbol{d}_n \leftarrow$ the optimal allocation of devices $\mathcal{D}$ using Algorithm 1, and initialize $\mathcal{D}'$ accordingly as the set of allocated devices of size $|\mathcal{D}'| = \min(D, MS)$
3: **while** $\mathcal{D}' \neq \varnothing$ **do**
4: Compute the power allocation $\boldsymbol{p}$ of devices set $\mathcal{D}'$ using (7)
5: **if** $\|\boldsymbol{p}\|_1 \leq P_{\max}$ **then**
6: $Z^* \leftarrow |\mathcal{D}'|$
7: **return** Z^*, $\boldsymbol{p}$ and $\forall n \in \mathcal{S}$, $\boldsymbol{d}_n$
8: **end if**
9: Remove $|\mathcal{D}'|$ from the device allocation $\boldsymbol{d}_n$, $n \in \mathcal{S}$
10: $\mathcal{D}' \leftarrow \mathcal{D}' \setminus \{|\mathcal{D}'|\}$
11: **end while**

Observe that since (7) calculates device power, the solution must always be positive. To ensure this, we see that the system has limitations on the admissible values of ζ and ξ. That is, if we wish to ensure that some specific data rate R should be achieved by all devices, we can tolerate only those values of ξ for which the solution to (7) is non-negative. This can be ensured by choosing a value of ξ for which the denominator of A^{-1} is positive. Alternatively, if we wish to ensure that the system can tolerate some specific residual interference ξ, we must choose a date rate R, and consequently the value of ζ, such that the denominator of A^{-1} is again positive.

This restriction is an implicit limitation of the NOMA system and can be better understood by studying the capacity region for devices in the NOMA system. For example, Fig. 1 shows the capacity region plot for a two-device $(M = 2)$ downlink NOMA system with imperfect SIC. The solid black lines represent the target data rate R for the devices. For this example, we have chosen $R = 25$ kbps. For both of the devices to be successfully connected, there must exist at least one point in the top right part of the intersection of the two solid black lines.

As shown by the curve in green, when $\xi < 1/\zeta^2$, which implies that A^{-1} is positive for the case of $M = 2$, there are some points which lie in the top right part of the intersection. This confirms the existence of a power allocation for the devices that will ensure that both the devices achieve a rate of

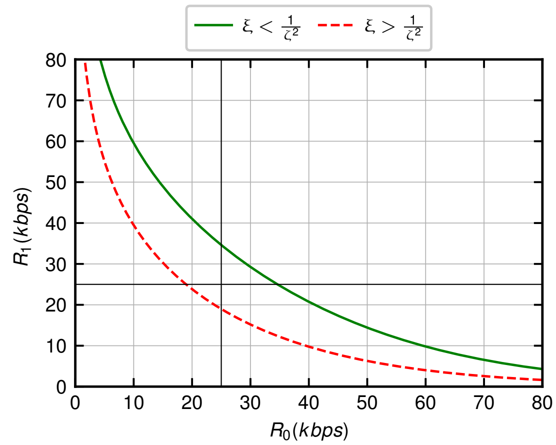

Fig. 1. Rate region plot for a two device NOMA system with imperfect SIC (R_0 and R_1 correspond to the achievable rates of the two devices respectively)

at least R kbps. However, when $\xi > 1/\zeta^2$, as shown by the red curve, there exists no value of power for the devices for which both of them can achieve a rate of R kbps or higher. Thus, at the very start of the allocation, before doing any device or power allocation, we can calculate a feasible value of M in the system, given ζ and ξ.

V. Simulation Results and Performance Evaluation

We analyze the performance of our proposed solution through computer simulations. The important system parameters are derived from 3GPP standards for NB-IoT [25]. The carrier frequency is taken to be 900 MHz with a system bandwidth of 180 kHz per PRB. Each sub-carrier has a bandwidth of 15 kHz. The value of AWGN is taken to be -174 dBm/Hz and the noise figure F is taken to be 5 dB. The distance dependent path-loss for a device at a distance of D meters from the BS is given as:

$$PL(D) = 120.9 + 37.6 \log \frac{D}{1000} + G,$$

where G is the antenna gain that is set to be -4 dB. We assume frequency flat, Rayleigh fading over the entire system bandwidth due to narrow-band consideration. Each PRB of 180 kHz bandwidth has 12 sub-carriers therefore the system can accommodate a maximum of 24 devices with $M = 2$ and 36 devices with $M = 3$, using a maximum of 23 dBm of power in any case. In all the simulations, we initially consider $M = 3$ in the system. The contending devices are dropped randomly following a uniform distribution in a hexagonal cell of radius 500 meters, unless otherwise stated. All results are averaged over 10000 independent runs.

Fig. 2 shows the variation of device power with the residual interference due to imperfect SIC. Here, we show results for only a single sub-carrier. We see that the effect of residual interference is more detrimental in the case of $M = 3$ when compared to that in $M = 2$. Additionally, the device with the weakest channel gain on a sub-carrier (d_1 for $M = 2$ and d_2 for $M = 3$) is the most affected by the increase in ξ as its power consumption increases the most.

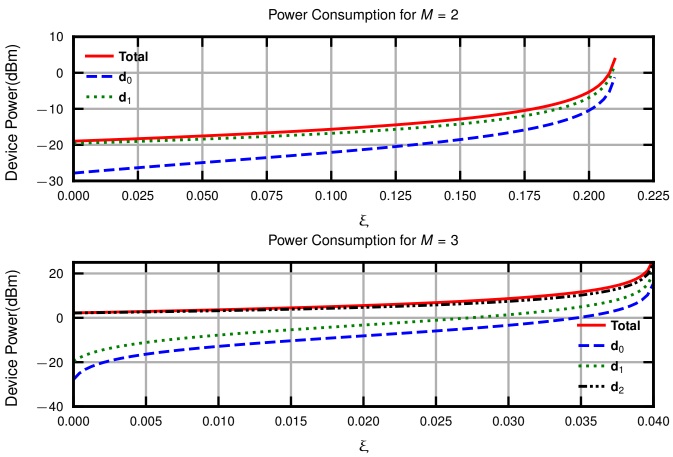

Fig. 2. Variation of the device power with residual interference, $R = 25$ kbps

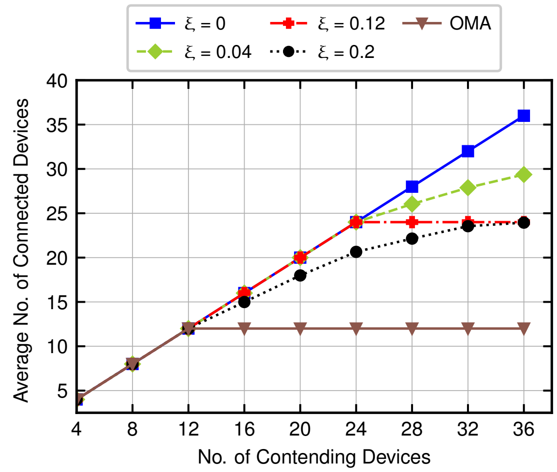

Fig. 3. Variation of the number of connected devices against the number of contending devices, $R = 25$ kbps

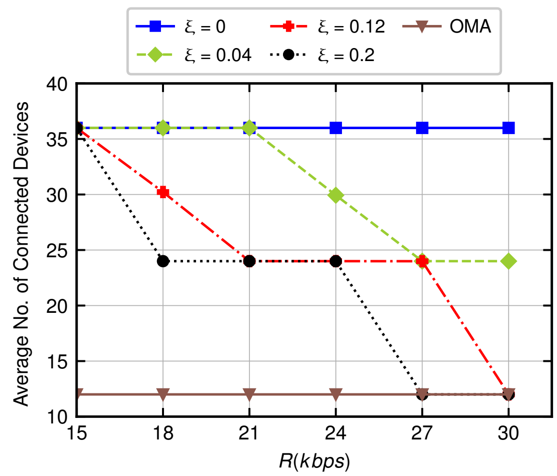

Fig. 4. Connectivity performance against different service rates

For the case of $M = 2$, the power required to connect the same devices increases by 5 dBm as ξ grows from 0 to 0.1 and by more than 20 dBm as ξ becomes 0.2. However, for $M = 3$ the required power grows 20 dBm when ξ become 0.04, i.e., 4% residual interference. This confirms the fact that in a practical system, we cannot expect to have a large number of superimposed devices per sub-carrier, since the power budget will get exhausted on a small number of devices with relatively small values of ξ such as 0.05.

In Fig. 3, we evaluate the number of connected devices in our NB-IoT NOMA system as the number of devices contending for connection increases. Here, R is set to be 25 kbps for all devices. When SIC is perfect, i.e., $\xi = 0$, all the 36 contending devices are successfully connected. However, as ξ increases to 0.04, the number of connected devices decrease by 18.41%. The connectivity falls by 33% when $\xi = 0.12$. In the case of $\xi = 0.2$, we see that the connectivity performance is poor even when we have fewer contending devices. For example, with 24 contending devices the system can accommodate only 20 devices on an average when $\xi = 0.2$. Another point to note that is when $\xi = 0.12$, we are able to connect no more than 24 devices even when more contending devices are available since. This behavior is in accordance to the discussion in Section IV since for the value of $\xi = 0.2$ and $\zeta = 2.174$ (corresponding to $R = 25$ kbps), $M = 3$ is infeasible for the system.

Fig. 4 presents the connectivity performance of the NOMA system with variation in the required service rate R. We see that in the case of perfect SIC, there is no impact on the connectivity performance of the algorithm as R increases from 15 kbps to 30 kbps. When $\xi = 0.04$, the connectivity starts decreasing after $R = 21$ kbps and the connectivity decreases by 16.84% when $R = 24$ kbps, and a further decrease of 33% when $R \geq 27$ kbps. For the case of $\xi = 0.12$, the connectivity goes down by 33.3% when R changes from 15 kbps to 24 kbps. When $\xi = 0.2$, the connectivity falls by 33.3% as R goes from 15 kbps to 18 kbps. The connectivity for $\xi = 0.2$ becomes even worse for $R \geq 27$ kbps, where only 12 devices can be connected in the system on an average. At high data rates ($R \geq 30$ kbps), the performance of the system with $\xi = 0.12$ and $\xi = 0.2$ is no better than that of an orthogonal multiple access (OMA) system, where each sub-carrier has only one device.

Additionally, we evaluate the performance of our proposed algorithm with different cell sizes. This heterogeneity in the cell radius is an important aspect of LPWAN deployments. We observe with the increase in the cell radius, lesser devices can be connected on an average due to the increased path-loss. When perfect SIC can be performed, the system suffers no degradation in connectivity as the cell radius grows from 250m to 1250m. However, as little as 4% of residual interference significantly affects the system and degrades the connectivity by 28.98% as the cell radius increases from 250 m to 750 m. With further increase in ξ, we see drastic fall in connectivity by 34.7% and 36.08% for $\xi = 0.12$ and 0.2 respectively as the cell radius increases from 250 m to 750 m. Furthermore, with $\xi = 0.2$ and a cell radius of 1250 m, the connectivity of the system becomes similar to that of an OMA system. This analysis consolidates the fact that systems with larger cell radius are more susceptible to performance degradation due to imperfect SIC.

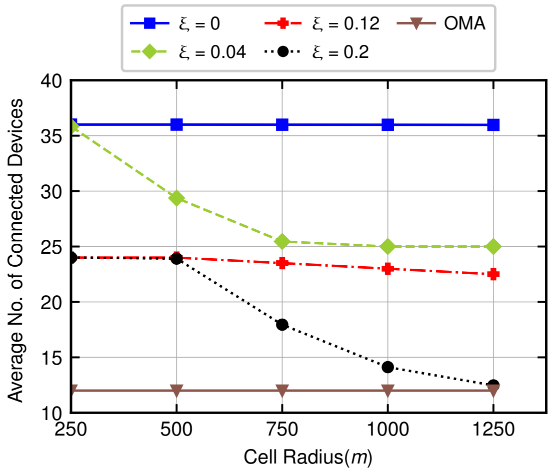

Fig. 5. Connectivity performance against different cell sizes, $R = 25$ kbps

VI. Conclusion

In this work, we investigate the problem of connection density maximization in the downlink for NB-IoT networks with residual interference due to imperfect SIC. We present a simple algorithm for the sub-carrier and power allocation that maximizes the device connectivity under this setting of imperfect SIC. Our iterative algorithm is based on solving a system of linear equations on each sub-carrier for power allocation, which is easy to implement and has low computational complexity. Through computer simulations, we study the performance of the proposed solution under various cell size and QoS requirement. Moreover, we show analytically that for a given value of ξ it is infeasible to accommodate large number of superimposed devices per sub-carrier as the service rate R increases. Over a wide range of service scenarios, we show that as low as 4% of residual interference from imperfect SIC can severely degrade the system's connectivity performance.

Acknowledgment

A part of the work has been carried out at the Laboratory for Information, Networking and Communication Sciences (www.lincs.fr), Paris.

References

[1] Cisco, "Cisco annual internet report (2018–2023)," Cisco, San Jose, CA, USA, Tech. Rep., March 2020.

[2] M. R. Palattella, M. Dohler, A. Grieco, G. Rizzo, J. Torsner, T. Engel, and L. Ladid, "Internet of things in the 5G era: Enablers, architecture, and business models," *IEEE JSAC*, vol. 34, no. 3, pp. 510–527, 2016.

[3] N. Xia, H. Chen, and C. Yang, "Radio resource management in machine-to-machine communications — A survey," *IEEE Communications Surveys & Tutorials*, vol. 20, no. 1, pp. 791–828, 2018.

[4] Y. . E. Wang, X. Lin, A. Adhikary, A. Grovlen, Y. Sui, Y. Blankenship, J. Bergman, and H. S. Razaghi, "A primer on 3GPP narrowband internet of things," *IEEE Commun. Mag.*, vol. 55, no. 3, pp. 117–123, 2017.

[5] H. Malik, J. L. R. Sarmiento, M. M. Alam, and M. A. Imran, "Narrowband-internet of things (NB-IoT): Performance evaluation in 5G heterogeneous wireless networks," in *IEEE International Workshop on Computer Aided Modeling & Design of Communication Links and Networks (CAMAD)*, 2019.

[6] N. Mangalvedhe, R. Ratasuk, and A. Ghosh, "NB-IoT deployment study for low power wide area cellular IoT," in *IEEE PIMRC*, 2016.

[7] K. Higuchi and A. Benjebbour, "Non-orthogonal multiple access (NOMA) with successive interference cancellation for future radio access," *IEICE Trans. on Commun.*, vol. E98.B, no. 3, pp. 403–414, 2015.

[8] L. Salaün, M. Coupechoux, and C. S. Chen, "Joint subcarrier and power allocation in NOMA: Optimal and approximate algorithms," *IEEE Transactions on Signal Processing*, vol. 68, pp. 2215–2230, 2020.

[9] Z. Zhang, Y. Hou, Q. Wang, and X. Tao, "Joint sub-carrier and transmission power allocation for MTC under power-domain NOMA," in *IEEE ICC Workshops*, 2018.

[10] Z. Ding, Z. Yang, P. Fan, and H. V. Poor, "On the performance of non-orthogonal multiple access in 5G systems with randomly deployed users," *IEEE Signal Proc. Letters*, vol. 21, no. 12, pp. 1501–1505, 2014.

[11] J. Kang and I. Kim, "Optimal user grouping for downlink NOMA," *IEEE Wireless Commun. Letters*, vol. 7, no. 5, pp. 724–727, 2018.

[12] M. B. Shahab, R. Abbas, M. Shirvanimoghaddam, and S. J. Johnson, "Grant-free non-orthogonal multiple access for IoT: A survey," *IEEE Commun. Surveys & Tutorials*, vol. 22, no. 3, pp. 1805–1838, 2020.

[13] A. Ikpehai, B. Adebisi, K. M. Rabie, K. Anoh, R. E. Ande, M. Hammoudeh, H. Gacanin, and U. M. Mbanaso, "Low-power wide area network technologies for internet-of-things: A comparative review," *IEEE Internet of Things Journal*, vol. 6, no. 2, pp. 2225–2240, 2019.

[14] A. E. Mostafa, Y. Zhou, and V. W. S. Wong, "Connection density maximization of narrowband IoT systems with NOMA," *IEEE Transactions on Wireless Communications*, vol. 18, no. 10, pp. 4708–4722, 2019.

[15] S. Mishra, L. Salaün, and C. S. Chen, "Maximizing connection density in NB-IoT networks with NOMA," in *IEEE VTC-Spring*, 2020.

[16] L. Bariah, A. Al-Dweik, and S. Muhaidat, "On the performance of non-orthogonal multiple access systems with imperfect successive interference cancellation," in *IEEE ICC Workshops*, 2018.

[17] S. Li, M. Derakhshani, and S. Lambotharan, "Outage-constrained robust power allocation for downlink MC-NOMA with imperfect SIC," in *IEEE International Conference on Communications (ICC)*, 2018.

[18] X. Li, J. Li, Y. Liu, Z. Ding, and A. Nallanathan, "Residual transceiver hardware impairments on cooperative NOMA networks," *IEEE Transactions on Wireless Communications*, vol. 19, no. 1, pp. 680–695, 2020.

[19] F. Cui, Z. Qin, Y. Cai, M. Zhao, and G. Y. Li, "Rethinking outage constraints for resource management in NOMA networks," *IEEE Journal of Selected Topics in Signal Proc.*, vol. 13, no. 3, pp. 423–435, 2019.

[20] Q. Lin and M. A. Weitnauer, "Practical residual interference after cancellation for constant envelope modulation with data-aided synchronization," *IEEE Access*, vol. 6, pp. 69 230–69 241, 2018.

[21] O. L. Alcaraz López, H. Alves, P. H. Juliano Nardelli, and M. Latva-aho, "Aggregation and resource scheduling in machine-type communication networks: A stochastic geometry approach," *IEEE Transactions on Wireless Communications*, vol. 17, no. 7, pp. 4750–4765, 2018.

[22] S. Mishra, L. Salaün, C. W. Sung, and C. S. Chen, "Downlink connection density maximization for NB-IoT networks using NOMA with perfect and partial CSI," *IEEE Internet of Things Journal*, 2021.

[23] D. Tse and P. Viswanath, *Fundamentals of Wireless Communication*. USA: Cambridge University Press, 2005.

[24] H. Wang, Z. Zhang, and X. Chen, "Energy-efficient power allocation for non-orthogonal multiple access with imperfect successive interference cancellation," in *International Conference on Wireless Communications and Signal Processing (WCSP)*, 2017.

[25] 3GPP, "Cellular system support for ultra-low complexity and low throughput Internet of Things (CIoT)," TR 45.820, Dec. 2015, v. 13.1.0. [Online]. Available: http://www.3gpp.org/DynaReport/45820.htm